Multidisciplinary Journal of TUM 4(2) 2025: 1-11 https://doi.org/10.48039/mjtum.v4i2.95 **Research Article**

Treatment of selected Halogenated Organic Compounds in Water using Colloidal Silver Nanocatalysts under Reducing Borohydride Conditions

Adan Tadicha*, Victor Wandera Opondo, Aloice Ogweno, Ali Shee

Department of Chemistry and Biological Sciences, Technical University of Mombasa, P.O. Box 90420-80100, Mombasa, Kenya

*Corresponding author's email: jilloadan@yahoo.com

Abstract

Halogenated organic compounds (HOCs) are frequently encountered water contaminants. They are widely used as solvents or feed stocks in the production of paints, adhesives, lacquerers, pharmaceuticals and veterinary drugs, cosmetics, pesticides and herbicides. Most HOCs are recalcitrant, toxic and possible carcinogens. HOCs treatment in water may involve physical, biological and chemical processes. Chemical treatment via oxidation or reduction processes are preferred due to their ability to transform HOCs into environmental benign products. Compared to reduction, oxidation may produce toxic byproducts and thus for complete mineralization, huge amounts of redox equivalents are needed. Reductive dehalogenation is selective and more suited for HOCs treatment. It may employ electrocatalysts, metal catalysts and reagents. Nanoscale zero valent iron (nZVI) as an electron-releasing reagent is environmentally compatible but ineffective for transformation of saturated aliphatic HOCs containing < 2 Cl-atoms. Noble metals such as Pt, Rh and Pd are excellent hydrogenation catalysts for HOCs reduction but are expensive and susceptible to deactivation in water. Metallic Ag (Ag^0) is a promising electrocatalyst for dechlorination of saturated aliphatic HOCs. Ag is relatively cheaper than the noble metals and is sparingly stable in water. Despite this potential, colloidal Ag^0 catalysts have received less attention for HOCs treatment. In this study, optimal conditions were established for synthesis of colloidal Ag^0 catalyst using sodium borohydride ($NaBH_4$). Calculated Ag^0 activities for reduction of dibromomethane, monobromomethane, perchloroethylene, trichloroethylene and vinylbromide were 86.92 ± 2.61, 3.45 ± 0.17, 2.38 ± 0.07, 1.16 ± 0.05 and 3.21 ± 0.10, respectively. The reduction of diclofenac and bromocresol blue by Ag^0+$NaBH_4$ was slow and incomplete due to catalyst deactivation. Thus, Ag^0+$NaBH_4$ is more appropriate for reduction of aliphatic and olefinic C—Cl and C—Br bonds.

Key Words: Colloidal silver nanocatalysts, Halogenated organic compounds, Reductive dehalogenation, Sodium borohydride, Water treatment

Introduction

Halogenated organic compounds (HOCs) are among the most frequently detected water and environmental contaminants. They are applied as important solvents and industrial feed stocks during the manufacture of pesticides, pharmaceuticals and veterinary drugs, paints, lacquerers, adhesives, cosmetics and household products (Kodavanti et al., 2023). Some low molecular weight HOCs found in water are referred to as disinfection byproducts (DBPs). DBPs are formed during the disinfection of waters containing natural organic matter by chlorine and chlorine derivatives. Due to their high chemical stability and poor biodegradability, these compounds tend to accumulate in the aquatic ecosystems hence posing significant ecological and human health risks, including endocrine disruption, genotoxic effects, and carcinogenicity (Vandana et al., 2022). HOCs are lipophilic hence undergo bioaccumulation and biomagnification in the food chain. The presence of HOCs has been

Published December 2025

reported in various water sources in Kenya, including rivers, lakes and municipal wastewater effluents, which shows the urgent need for effective and sustainable water treatment strategies (Chepchirchir et al., 2024).

Currently, adsorption of HOCs from water onto various sorbents are the most common. Adsorption only transfers the contaminant onto a solid phase where further treatment is needed. Regeneration of sorbents by strong acids and alkali results to production of huge amounts of sludge as well as sorbent losses. Compared to adsorption, oxidation of HOCs may lead to detoxification. However, oxidation reactions tend to produce toxic halogenated byproducts which are sometimes more toxic than the parent HOCs. Thus, for complete mineralization of the toxic halogenated byproducts, huge amounts of redox equivalents are consumed. Compared to oxidation, reduction of HOCs is more selective and leads to significant detoxification. Since reduction is selective (R—X + reducing agent → R—H+X^-), less redox equivalents are needed to accomplish detoxification. In most cases, reduction at ambient environmental conditions results in transformation of HOCs into benign products but not to full mineralization. Thus, coupling reductive processes with biological follow up treatment might be necessary. Reduction of HOCs in water by metals under anoxic conditions is a promising method, both at laboratory and field scales. Reduction may be facilitated by electrocatalysts, metallic reagents and metal catalyst. Electrocatalytic reduction of HOCs at metal cathodes may be mediated by electrons or surface adsorbed H-species. However, electrocatlytic reduction of HOCs in water is limited to < -1.2 V cathodic potentials. Further increase in cathodic potentials reduces efficiency due to the undesired water electrolytic reaction.

Metallic reagents such as nanoscale zero valent iron (nZVI) as electron-transmitting reagents are more suitable for *in situ* HOCs treatment. nZVI is environmentally compatible and easily injectable into subsurface systems. Nevertheless, drawbacks to nZVI include extremely low reaction rates for saturated aliphatic HOCs, its consumption over time, high corrosion tendency and generation of iron-oxide sludge in the presence of oxygen. Noble metal catalysts in combination with H_2 or H-donors offer higher HOCs reactivity than nZVI. Although noble metals such as Rh, Pd and Pt offer high activity for HOCs transformation, they are expensive and readily undergo surface fouling deactivation in water. Recently, Cu catalysts in combination with sodium borohydride ($NaBH_4$) have been found to offer an alternative to Pd/H_2 system. Under identical conditions, Cu+$NaBH_4$ showed high activity for reduction of saturated aliphatic HOCs than Pd/H_2 system. Although Ag belongs to the same group as Cu in the periodic table, it has received less attention in reductive dehalogenation reactions. Bulk Ag as a cathode has been applied to dechlorination of chlorinated methanes and ethanes. Shee et al., (2022) observed that compared to Cu, Ag nanocatalysts with $NaBH_4$ showed better selectivity to methane during transformation of chloroform. These results although limited show the potential of Ag as a heterogeneous catalyst in reductive dehalogenation reactions. Similar to Cu, Ag is less active for activation of H_2 into activated H-species. Thus, a strong reducing agent such as $NaBH_4$ is needed. This study provides a deeper understanding on the application of Ag+$NaBH_4$ by providing information regarding optimal synthesis conditions, classes of C—X bonds that could be cleaved and catalytic activities for a selected HOCs. The performance of Ag+$NaBH_4$ was assessed by selected HOCs classes representing saturated aliphatic, olefinic and aromatic HOCs. This study then compares Ag+$NaBH_4$ with other commonly used reduction systems to recommend application areas.

Materials and Methods

Materials, chemicals and reagents

All reagents used were of analytical grade. $NaBH_4$ was purchased from SRL, silver nitrate ($AgNO_3$) from REFCHEM, diclofenac and bromocresol blue were supplied by BDH Chemicals. Trichloroethylene (TCE), perchloroethylene (PCE), dibromomethane

Published December 2025

(DBM), monobromomethane (MBM), and vinyl bromide (VB) were sourced from Sigma-Aldrich, Germany.

Synthesis of AgNPs

A 60 mL aqueous solution of $AgNO_3$ (0.001-0.002 M) was prepared in a 120 mL glass vial. The pH of the solution was adjusted to 10 using 0.1 M NaOH followed by addition of alkaline $NaBH_4$ (0.00025-0.004 M) under constant stirring in a fume hood. Stirring was continued for 30 min to allow nucleation and growth of the nanoparticles. The formation of AgNPs was monitored by measuring their surface plasmon resonance (SPR) from 400-800 nm using a UV-VIS spectrophotometer (UV1700). The AgNPs were stored in sealed glass vials under inert conditions for further analysis.

Batch dehalogenation experiments

Batch reactors consisted of 120 mL serum bottles sealed with Teflon butyl rubber septa and aluminum crimp caps. The aqueous phase for volatile and non-volatile HOCs were 60 mL and 100 mL, respectively. The degradation of each parent HOC was carried out under ambient conditions. A fixed concentration of AgNPs were prepared and a methanol extract of the HOC was spiked to initiate reaction. Headspace analysis was applied for volatile HOCs (MBM, DBM, PCE, TCE and VB) while aqueous phase analysis was used for the non-volatile, DFN and BCB. HOCs degradation studies were monitored by gas chromatography mass spectrometry (GC-MS). A 25 µL headspace was extracted using a gas-tight syringe at each sampling point then analyzed by GC-MS. For DFN and BCB, 1 mL was extracted and analyzed using UV-VIS spectrophotometry (UV 1700) at fixed λ_{max}. The concentrations of HOCs and their degradation products were quantified using external calibration curves. Under identical conditions, control experiments were conducted by mixing the parent HOC separately with distilled water, $AgNO_3$ and $NaBH_4$. All experiments were performed in triplicate and the results presented as mean ± SD.

Analytical methods

Analysis of HOC as educts and degradation products were performed by GC-MS (GC2010, Shimadzu) coupled with MS (GCMS-QP2010, Shimadzu). Gas chromatography was fitted with a DB-1ms capillary column (J & W, 60 m x 0.25 mm x 0.25 µm). The temperature conditions for the oven, interface, injector port, and detector were set at 180, 40, 200 and 250 °C, respectively. For headspace sampling of aliquots for GC analysis, a 25 µL gastight syringe was used, where the split ratio was set to 5. For better GC-MS sensitivity, the total ion count for each HOC substance were applied. The analysis of hydrocarbons was done using a gas chromatography (GC 2010 Plus, Shimadzu) equipped with a flame ionization detector (FID). The GC was fitted with a wide bore capillary column (GS-Q, 30 m x 0.53 mm x 1.00 µm) whose temperature conditions were set at 200, 40 and 280 °C for the injector, oven and detector, respectively. A 25 µL gastight glass syringe was also used for headspace hydrocarbon sampling for GC analysis and the split ratio was also set at 5. Using calibration curves, the external standard approach was applied to calculate the concentration of parent HOC as educt and degradation products. Due to change in headspace volume by H_2 production from $NaBH_4$, propane was added in the reactor as an internal standard. Upon ≥ 95% conversion of the parent HOCs and their halogenated intermediates, the amount of Cl^- or Br^- were determined by ion chromatography (IC25, Dionex, IonPac AS15/AG15) equipped with a conductivity detector and self-regenerating suppressor. The amount of Cl^- or Br^- (X_q) was calculated using equation 1:

$$Xq = \frac{Xm}{Xt} x\ 100 \quad (1)$$

Where X_q is the percent yield of Cl^- or Br^-, X_m is the amount of Cl^- or Br^- and X_t represent the theoretical maximum amount of Cl^- or Br^- when the parent HOC is completely dehalogenated. The amount of AgNPs and HOCs were adjusted to prevent oversaturation of surface-active centers and allow the reaction to follow pseudo-first-order kinetics as given by equation 2:

$$\frac{dC}{dt} = -k_{obs}C \quad (2)$$

Where c is the concentration of HOC (mg/L) and k_{obs} is the pseudo-first-order rate constant (/min). To compare the reactivities of the HOCs under the given reaction conditions, the catalytic activities for metallic Ag (A_{Ag}) were calculated using equation 3:

$$A_{Ag} = \frac{k_{obs}}{\ln 2 \cdot c_m} \quad (3)$$

Also, the value of A_{Ag} can be calculated using equation 4:

$$A_{Ag} = \frac{1}{c_m \cdot \tau_{1/2}} \quad (4)$$

Where $\tau_{1/2}$ is the HOC half-life of the reaction (min) obtained from the HOC reduction profile.

Results and Discussion

Optimal conditions for synthesis of AgNPs using $NaBH_4$

$NaBH_4$ ($E°$ = -1.24 V vs Standard Hydrogen Electrode (Njoya et al., 2024)) is a strong reductant that readily reduces most metal ions to their metallic states e.g., Ag^+ to Ag^0 (Silva & and Cesarino, 2022) . Under identical reaction conditions it has been found the amount of $NaBH_4$ and precursor ($AgNO_3$) controls the size, particle distribution and surface morphology of the nanoparticles produced (Villaverde et al., 2021). A high initial concentration of $NaBH_4$ result to rapid nanoparticles formation. However, rapid reaction produces large and non-uniform nanoparticles (Šutka et al., 2024). A low concentration of $NaBH_4$ result to incomplete nanoparticles formation (Saini et al., 2022). Thus, establishing optimal reaction conditions is necessary to produce nanoparticles of desired sizes, particle distribution and surface morphology. These properties are crucial in determining catalytic activities. In many heterogeneous catalytic reactions, smaller and uniformly sized nanoparticles are preferred due to their high inherent activities. To establish optimal reaction conditions, concentrations of $NaBH_4$ were varied from 0.00025 to 0.004 M at fixed concentrations of $AgNO_3$ (0.001 M). The appearance of the resultant solutions containing AgNPs are shown in Figure 1 where the colour of the solutions changes from deep yellow at high NaBH4 concentration (0.004 M) to light yellow at low NaBH4 concentration (0.00025 M).

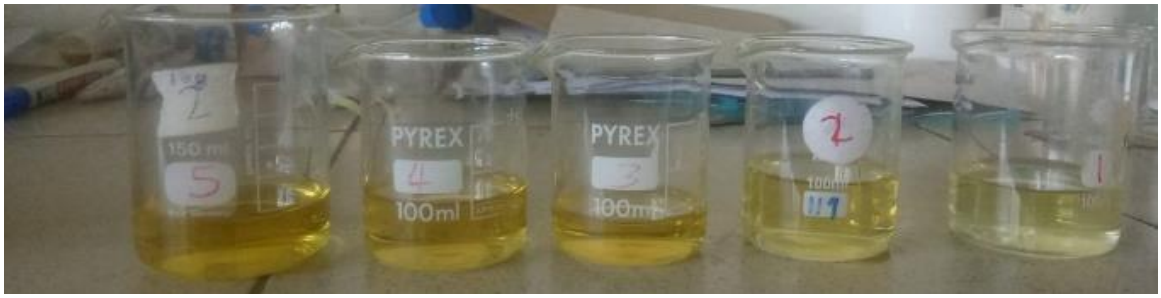

Figure 1. Appearance of the solutions of AgNPs upon reduction of 0.001 M $AgNO_3$ as $NaBH_4$ concentration decreases from 0.004 to 0.00025 M (left to right)

Table 1 shows the λmax and absorbance values of the resultant solutions containing AgNPs at the range of 400-450 nm indicating the presence of AgNPs (Tamilselvan et al., 2022).

Table 1. Variation in λ_{max} for AgNPs produced at different $NaBH_4$ concentrations (pH_0 = 10, c_{AgNO3} = 0.001M)

$AgNO_3$ (M)	$NaBH_4$ (M)	λ_{max} (nm)	Absorbance
0.001	0.00025	415.4	0.087
0.001	0.00050	412.2	0.179
0.001	0.00100	407.6	0.374
0.001	0.00200	406.6	0.298
0.001	0.00400	405.4	0.443

It has been found that the size, shape and distribution of AgNPs influences position and intensity of SPR peaks (Zein et al., 2022). SPR peaks within 400-450 nm range suggest the formation of spherical-shaped AgNPs (Jameel et al., 2022). As shown in Table 1, the change in λ_{max} as concentration of $NaBH_4$ changes is an indication to change in AgNPs sizes. A red shift, defined as a shift of the λ_{max} peak to longer wavelengths, implies formation of larger AgNPs. A blue shift towards shorter λ_{max}, indicates formation of smaller spherical AgNPs (Sørensen et al., 2022). A higher absorbance implies increased concentrations of AgNPs or an increased average particle size (Bélteky et al., 2021). When $NaBH_4$ is 0.00025M the λ_{max} is large (415.4 nm) while the absorbance is low implying slow reduction reaction producing larger nanoparticles. It also implies fewer nucleation sites due to incomplete reduction of Ag^+ and, hence, a lower concentration of nanoparticles (Szczyglewska et al., 2023). As the concentration of $NaBH_4$ is increased to 0.001 M, a blue shift in λ_{max} is observed indicating a decrease in the AgNPs sizes and higher concentration of nanoparticles with uniform particle sizes and distribution. This further implies that at a higher concentration of $NaBH_4$, efficient reduction of Ag^+ occurs, resulting in more nucleation sites and smaller nanoparticles (Zhou et al., 2022). However, at the highest $NaBH_4$ concentration of 0.004 M, there is minimal decrease in λ_{max} an indication that saturations occur and further addition of the reductant has minimal effect on the size and concentration of the produced AgNPs. The excess reductant could be essential in maintaining the nanoparticles in their reduced state. As shown in Table 1, a molar ratio of 1:1 for $AgNO_3$ and $NaBH_4$ produces smaller nanoparticles, λ_{max} = 407.6 nm with a higher absorbance. Further increase in reductant concentration has minimal effect on λ_{max} and thus nanoparticle sizes and distribution. Thus, a molar ratio of 1:1 for $AgNO_3$ and $NaBH_4$ is ideal to produces smaller and uniform AgNPs.

Dehalogenation activities of colloidal AgNPs under reducing $NaBH_4$ conditions for selected HOCs classes

Reductive dehalogenation reactions are usually sensitive to the strength of C—X bond as well the chemical environment adjacent to the C—X bond. For example, Pd/H_2 system shows higher activities during the reduction of C—Cl and C—Br attached to olefinic and aromatic systems. However, Pd activities are very low for saturated aliphatic C—Cl bonds. Similarly, nZVI shows higher activities for highly chlorinated compounds but fails for C—Cl bonds attached to aromatic structures. It is noteworthy to point out that both Pd and nZVI fail to reduce saturated aliphatic compounds containing ≤ 2 Cl atoms. Recently, it was established that Cu activities were higher for saturated aliphatic C—Cl and C—Br bonds. In addition, Cu also readily dechlorinates saturated aliphatic compounds containing ≤ 2 Cl atoms. Nevertheless, Cu activities are low for C—Cl attached to olefinic and aromatic structures. In order to determine the type of C—Cl and C—Br bonds that could be reduced by AgNPs under reducing $NaBH_4$ conditions, the following HOCs were evaluated: DBM, MBM, PCE, TCE, VB, DFN and BCB. These compounds were selected as representatives for the different classes of HOCs frequently encountered in water and the environment. DBPs are common water contaminants which need constant monitoring and treatment before natural waters could be used for drinking or recreation. As stated earlier, AgNPs with $NaBH_4$ readily reduces C—Cl bonds in chlorinated alkyls (Wu et al., 2024). A potential application of AgNPs in reduction of other classes of DBPs and halogenated alkyls was studied with the knowledge that Br^- is a known catalyst deactivator (Sun et al., 2023). The A_{Ag} for selected HOCs and their transformation products are shown in Table 2.

Table 2. Calculated A_{Ag} for reduction of selected HOCs in water

HOC substance	Weakest Bond Dissociation Energy (BDE) (kJ/mol)	A_{Ag} (L/(g.min)	Cl^- or Br^- yield (%)	Final Products (%)
DBM	276 (King & Mitch, 2022)	86.92±2.61	96±3	CH_4(98) C_2H_6(<1%)
MBM	294 (Bajec et al., 2020)	3.45±0.17	98±2	CH_4(98), C_2H_6(<1)
PCE	382 (Zheng et al., 2024)	2.38±0.07	95±4	C_2H_6(13) C_2H_4(85%)
TCE	392 (Brumovský et al., 2022)	1.16±0.05	95±3	C_2H_6(10%) C2H_4(88%)
VB	338 (Pagire et al., 2020)	3.2±0.10	98±2	C_2H_6(4%) C_2H_4(94%)

Cl^- and Br^- yield calculated at > 95% of parent HOC and its dehalogenated intermediates. Final products yield calculated at > 95% of parent HOC and its dehalogenated intermediates

Dehalogenation of DBM and MBM in water was performed and the calculated A_{Ag} for reduction of DBM and MBM are 86.92 ± 2.61 and 3.45 ± 0.17 L/(g.min), respectively. For the two compounds, the ease of dehalogenation depends on the strength of C—Br bond (Table 2). Therefore, DMB is readily reduced than MBM. Since the reaction proceeded to completion, colloidal Ag^0 showed great tolerance to residual Br^- released during the reaction. Similar to the reduction of DBM and MBM, the ease of dechlorination for PCE and TCE was dependent on the C—Cl bond strength. As shown in Table 2, the calculated A_{Ag} for dechlorination of PCE and TCE were 2.38 ± 0.07 and 1.16 ± 0.05 L/(g.min), respectively. Therefore, PCE with a weaker BDE is readily dechlorinated than TCE. However, the A_{Ag} for PCE and TCE are within the same order of magnitude, implying that BDE is not the only factor controlling reaction rates for olefinic compounds at Ag surfaces, other factors may as well be controlling the reduction process.

In many heterogeneous catalytic reactions, both adsorption and dehalogenation processes control HOCs reactivity (Weidlich, 2021). Metal nanocatalysts strongly interact with compounds containing π-systems. The olefinic compound adsorption via π—π interactions onto active sites on the metal surface precedes dechlorination reactions. Thus, non-destructive adsorption may not be correlated with weakest BDE (Jarosiewicz et al., 2020). As shown in Table 2, the calculated A_{Ag} activity for reduction of VB in water is 3.21 ± 0.10 L/(g.min). Although the A_{Ag} value for VB is higher than for both PCE and TCE (Table 2), it is within the same order of magnitude. Thus, a clear indication that the reduction of olefinic HOCs follows a similar mechanism and the strength of C—X bond plays only a minor role.

In order to evaluate the ability of AgNPs with $NaBH_4$ to reduce aromatic C—Cl and C—Br bonds, DFN and BCB were selected as test substances. DFN is a common water contaminant while BCB was selected as representative for brominated flame retardants. Dehalogenation of DFN and BCB were carried in this study and the time profiles are presented in Figures 2 and 3 for DFN and BCB, respectively.

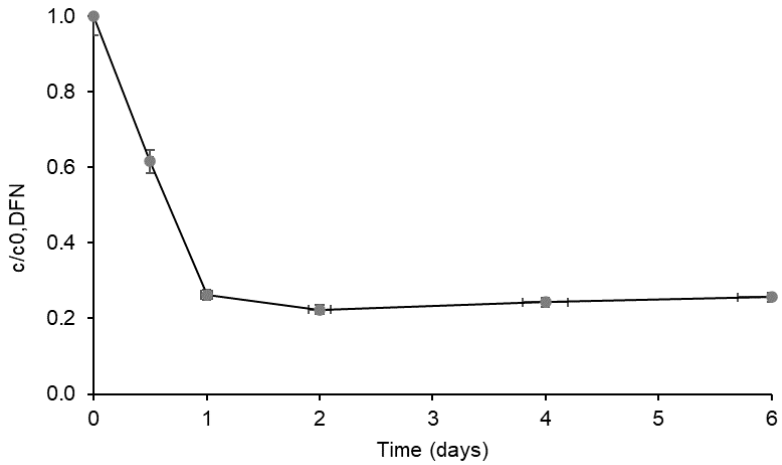

Figure 2. Reaction profile for the dechlorination of DFN using colloidal AgNPs under reducing $NaBH_4$ conditions (c_{AgNPs} = 2500 mg/L; $c_{0,NaBH4}$ = 3000 mg/L; $c_{0,DFN}$ = 10 mg/L; Cl^- yield = 60 ± 5%)

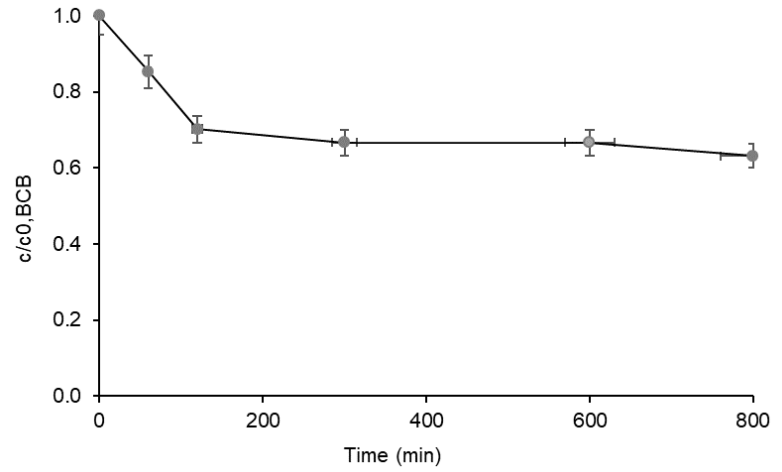

Figure 3. Reaction profile for the dehalogenation of BCB using colloidal AgNPs under reducing NaBH4 conditions (cAgNPs = 2500 mg/L; c0,NaBH4 = 3000 mg/L; c0,BCB = 10 mg/L; Br- yield = 20 ± 5%)

From Figures 2 and 3, the reduction of DFN and BCB was incomplete. After 24 h, conversion of DFN was about 74% while that of BCB was only 20-25%. Further addition of $NaBH_4$ had no effect on the reduction of DFN and BCB, possible due to deactivation of the catalysts. Shee et al., (2022) demonstrated that for fast reacting substances like $CHCl_3$, AgNPs were tolerant to Cl^- released during the reaction. Since, DFN and BCB have complex aromatic structures compared to the C_1 and C_2 compounds investigated in this study, there adsorption on AgNPs through π−π interactions could block and thus deactivate available surface-active sites. Nevertheless, this is open for further investigation. The deactivation of AgNPs catalysts due to chemical structures of parent HOC molecules and their byproducts although interesting was not part of this study.

Comparison of reduction abilities of AgNPs+$NaBH_4$ with nZVI, CuNPs+$NaBH_4$ and Pd+H_2 for selected HOCs in water

In the remediation of water and environmental compartments contaminated with HOCs, the most common reduction systems utilize nZVI as an electron transmitting reagent and Pd catalysts in combination with H_2 (Gong et al., 2022). Recently Cu^0+$NaBH_4$ was also investigated (Shee et al., 2022). The results obtained for the dehalogenation abilities of Ag^0+$NaBH_4$ were

compared with those of Cu, nZVI and Pd catalysts using DBM, MBM, PCE, TCE and VB as test substances. The results are presented in Table 3.

Table 3. Comparison of catalytic activities of Ag,Cu, nZVI and Pd for selected HOCs under identical conditions

HOC substance	A_m **(L/(g.min)**			
	m= Ag	**m= Cu**	**m= nZVI**	**m= Pd**
DBM	86.92±2.61	390±20 (Shee et al., 2022)	0.03±0.01 (Shee et al., 2022)	40±10 (Mackenzie, 2022)
MBM	3.45±0.17	20±3 (Shee et al., 2022)	n.a	n.a
PCE	2.38±0.07	3±1 (Shee et al., 2022)	0.00040±0.00022 (Shee et al., 2022)	110±10 (Mackenzie, 2022)
TCE	1.16±0.05	17±1 (Shee et al., 2022)	0.00024±0.00004 (Shee et al., 2022)	220±50 (Mackenzie, 2022)
VB	3.21±0.10	67±10 (Shee et al., 2022)	0.0028±0.0002 (Shee et al., 2022)	2500±500 (Mackenzie, 2022)

n.a = not analyzed

As shown in Table 3, Cu shows better catalytic activities for reduction of saturated aliphatic HOCs than Ag. Since Ag is expensive than Cu and that A_{Cu} is higher than A_{Ag}, Cu^0+$NaBH_4$ could be best for reduction of saturated aliphatic HOCs. Although Pd+H_2 shows higher activities for reduction of the olefinic HOCs than all the other systems, it is expensive and readily deactivated by macromolecules e.g., NOM and ionic solutes e.g., SO_3^{2-} and S^{2-}. Thus, Pd usage is also limited to water that has been pre-treated to remove deactivators (macromolecules and ionic solutes) which are ubiquitous in water and the environment. These deactivators poison Pd making it inactive. Since nZVI is environmentally compatible, it is best for *in situ* treatment of groundwater contaminated with HOCs. For treatment of industrial wastewaters contaminated with HOCs within a short period of contact time, Cu^0+$NaBH_4$ should be considered.

Conclusions

Optimal process conditions for synthesis of colloidal AgNPs catalysts using $NaBH_4$ are 0.001M $AgNO_3$ and 0.001M $NaBH_4$. Calculated A_{Ag} for the reduction of DBM, MBM, PCE, TCE and VB using colloidal AgNPs catalysts and $NaBH_4$ at pH0 = 10 were 86.92 ± 2.61, 3.45 ± 0.17, 2.38 ± 0.07, 1.16 ± 0.05 and 3.21 ± 0.10 (L/(g.min), respectively. DBM and MBM were readily dehalogenated with high A_{Ag} activities dependent on strength of C—Br bond. Dehalogenation of olefinic substances PCE, TCE and VB showed lower A_{Ag} activities than for the brominated methanes. Also, the A_{Ag} activities for PCE, TCE and VB were within the same order of magnitude implying a similar reduction mechanism and the strength of the weakest C—Cl and C—Br bond is not the only factor controlling the dehalogenation reaction. Comparison of Ag activities with those of Cu, Pd and nZVI were done to recommend application areas as follows: Cu^0+$NaBH_4$ is to be considered for treatment of saturated aliphatic HOCs in water and olefinic HOCs present in industrial waters and wastewater. nZVI as an environmentally compatible electron-transmitting reagent is more appropriate for *in situ* treatment of HOCs contaminated groundwater. Since Ag is more expensive than Cu and readily deactivated in water, AgNPs+$NaBH_4$ may find less application in the treatment of water contaminated with HOCs.

Acknowledgements

We are grateful to the Kenya Petroleum Refineries Limited for funding this study, and the Government Chemists, Mombasa for providing laboratories for analysis.

References

Bajec, D., Grom, M., Lašič Jurković, D., Kostyniuk, A., Huš, M., Grilc, M.,

Likozar, B., & Pohar, A. (2020). A Review of Methane Activation Reactions by Halogenation: Catalysis, Mechanism, Kinetics, Modeling, and Reactors. *Processes*, 8(4). https://doi.org/10.3390/pr8040443

Bélteky, P., Rónavári, Andrea, Zakupszky, Dalma, Boka, Eszter, Igaz, Nóra, Szerencsés, Bettina, Pfeiffer ,Ilona, Vágvölgyi, Csaba, Kiricsi, Mónika, & Kónya, Z. (2021). Are Smaller Nanoparticles Always Better? Understanding the Biological Effect of Size-Dependent Silver Nanoparticle Aggregation Under Biorelevant Conditions. *International Journal of Nanomedicine*, 16(null): 3021–3040 https://doi.org/10.2147/IJN.S304138

Brumovský, M., Oborná, J., Micić, V., Malina, O., Kašlík, J., Tunega, D., Kolos, M., Hofmann, T., Karlický, F., & Filip, J. (2022). Iron Nitride Nanoparticles for Enhanced Reductive Dechlorination of Trichloroethylene. *Environmental Science & Technology*, 56(7): 4425–4436 https://doi.org/10.1021/acs.est.1c08282

Chepchirchir, R., Mwalimu, R., Tanui, I., Kiprop, A., Krauss, M., Brack, W., & Kandie, F. (2024). Occurrence, removal and risk assessment of chemicals of emerging concern in selected rivers and wastewater treatment plants in western Kenya. *Science of The Total Environment*, 948: 174982. https://doi.org/10.1016/j.scitotenv.2024.174982

Gong, L., Zhang, Z., Xia, C., Zheng, J., Gu, Y., & He, F. (2022). A quantitative study of the effects of particle' properties and environmental conditions on the electron efficiency of Pd and sulfidated nanoscale zero-valent irons. *Science of The Total Environment*, 853: 158469. https://doi.org/10.1016/j.scitotenv.2022.158469

Jameel, M.S., Aziz, A.A., Dheyab, M.A., Khaniabadi, P.M., Kareem, A.A., Alrosan, M., Ali, A.T., Rabeea, M.A., & Mehrdel, B. (2022). Mycosynthesis of ultrasonically-assisted uniform cubic silver nanoparticles by isolated phenols from Agaricus bisporus and its antibacterial activity. *Surfaces and Interfaces*, 29: 101774. https://doi.org/10.1016/j.surfin.2022.101774

Jarosiewicz, M., Miłowska, K., Krokosz, A., & Bukowska, B. (2020). Evaluation of the Effect of Selected Brominated Flame Retardants on Human Serum Albumin and Human Erythrocyte Membrane Proteins. *International Journal of Molecular Sciences*, 21(11) https://doi.org/10.3390/ijms21113926

King, J.F., & Mitch, W.A. (2022). Electrochemical Reduction of Halogenated Alkanes and Alkenes Using Activated Carbon-Based Cathodes. *Environmental Science & Technology*, 56(24): 17965–17976 https://doi.org/10.1021/acs.est.2c05608

Kodavanti, P.R.S., Costa, L.G., & Aschner, M. (2023). Chapter One—Perspective on halogenated organic compounds. In P. R. S. Kodavanti, M. Aschner, & L. G. Costa (eds.), *Neurotoxicity of Halogenated Organic Compounds* Vol. 10: 1–25 Academic Press. https://doi.org/10.1016/bs.ant.2023.06.001

Mackenzie, K. (2022). Metallic Copper as Dehalogenation Catalyst in the Treatment of Water and Wastewaters. In D. Fernández González & L. F. Verdeja González (eds.), *Copper – From the Mineral to the Final Application*. IntechOpen.

https://doi.org/10.5772/intechopen.108147

Njoya, O., Pam, S., & Oyono, J.S.O. (2024). Suitability of cyclic voltammetry for the measurement of sodium borohydride (NaBH4) in a solution of Cr(VI)/organic compounds/NaBH4. *Water Practice and Technology*, 19(7): 2920–2928 https://doi.org/10.2166/wpt.2024.174

Pagire, S.K., Föll, T., & Reiser, O. (2020). Shining Visible Light on Vinyl Halides: Expanding the Horizons of Photocatalysis. *Accounts of Chemical Research*, 53(4): 782–791 https://doi.org/10.1021/acs.accounts.9b00615

Saini, B., Khamari, L., & Mukherjee, T.K. (2022). Kinetic and Mechanistic Insight into the Surfactant-Induced Aggregation of Gold Nanoparticles and Their Catalytic Efficacy: Importance of Surface Restructuring. *The Journal of Physical Chemistry B*, *126*(10), 2130–2141. https://doi.org/10.1021/acs.jpcb.2c00702

Shee, A., Kopinke, F.D., & Mackenzie, K. (2022). Borohydride and metallic copper as a robust dehalogenation system: Selectivity assessment and system optimization. *Science of The Total Environment*, 810: 152065 https://doi.org/10.1016/j.scitotenv.2021.152065

Silva, M.K.L., & Cesarino, I. (2022). Electrochemical sensor based on Sb nanoparticles/reduced graphene oxide for heavy metal determination. *International Journal of Environmental Analytical Chemistry*, 102(13): 3109–3123. https://doi.org/10.1080/03067319.2020.1763973

Sørensen, L.K., Khrennikov, D.E., Gerasimov, V.S., Ershov, A.E., Polyutov, S.P., Karpov, S.V., & Ågren, H. (2022). Nature of the Anomalous Size Dependence of Resonance Red Shifts in Ultrafine Plasmonic Nanoparticles. *The Journal of Physical Chemistry C*, 126(39): 16804–16814. https://doi.org/10.1021/acs.jpcc.2c03738

Sun, C., Wen, R., Qin, Y., Wang, L., Wang, Y., Dou, M., & Wang, F. (2023). Origin of Pt Site Poisoning by Impurities for Oxygen Reduction Reaction Catalysis: Tailored Intrinsic Activity of Pt Sites. *ACS Applied Energy Materials*, *6*(11): 5700–5709. https://doi.org/10.1021/acsaem.3c00027

Šutka, A., Bitina, S., Smits, K., Šutka, A., Bikse, L., Maiorov, M., Käämbre, T., Timusk, M., Laipniece, L., & Lazdovica, K. (2024). Rapid, high-yield aqueous synthesis of ultrafine magnetite nanoparticles from Fe(III) precursor at room temperature. *Journal of Materials Science*, 59(2): 447–457 https://doi.org/10.1007/s10853-023-09233-5

Szczyglewska, P., Feliczak-Guzik, A., & Nowak, I. (2023). Nanotechnology–General Aspects: A Chemical Reduction Approach to the Synthesis of Nanoparticles. *Molecules*, 28(13) https://doi.org/10.3390/molecules28134932

Tamilselvan, S., Soniya, R.M., Vasantharaja, R., Kannan, M., Supriya, S., Batvari, B.P.D., Ramesh, T., & Govindaraju, K. (2022). Silver nanoparticles based spectroscopic sensing of eight metal ions in aqueous solutions. *Environmental Research*, 212: 113585 https://doi.org/10.1016/j.envres.2022.113585

Vandana, Priyadarshanee, M., Mahto, U., & Das, S. (2022). Chapter 2—

Mechanism of toxicity and adverse health effects of environmental pollutants. In S. Das & H. R. Dash (Eds.), *Microbial Biodegradation and Bioremediation (Second Edition)* (Second Edition, pp. 33–53). Elsevier. https://doi.org/10.1016/B978-0-323-85455-9.00024-2

Villaverde, Laurenti, M., Rubio-Retama, J., & Contreras-Cáceres, R. (2021). Reducing Agents in Colloidal Nanoparticle Synthesis – an Introduction. In S. Mourdikoudis (Ed.), *Reducing Agents in Colloidal Nanoparticle Synthesis* (p. 0). The Royal Society of Chemistry. https://doi.org/10.1039/9781839163623-00001

Weidlich, T. (2021). The influence of copper on halogenation/dehalogenation reactions of aromatic compounds and its role in the destruction of polyhalogenated aromatic contaminants. *Catalysts*, *11*(3), 378.

Wu, H., Chen, L., Tang, C., Fan, X., Liu, Q., & Xu, Y. (2024). Silver nanoparticles catalyzed electrochemical hydrodechlorination of dichloromethane to methane in N,N-Dimethylformamide using water as hydrogen donor. *Separation and Purification Technology*, *331*, 125647. https://doi.org/10.1016/j.seppur.2023.125647

Zein, R., Alghoraibi, I., Soukkarieh, C., Ismail, M. T., & Alahmad, A. (2022). Influence of Polyvinylpyrrolidone Concentration on Properties and Anti-Bacterial Activity of Green Synthesized Silver Nanoparticles. *Micromachines*, *13*(5). https://doi.org/10.3390/mi13050777

Sun Y., Zheng K., Du X., Qin H., Guan X.rt (2024). Insights into the contrasting effects of sulfidation on dechlorination of chlorinated aliphatic hydrocarbons by zero-valent iron. *Water Research*, 255: 121494.https://doi.org/10.1016/j.watres.2024.121494

Zhou, F., Zhu, Y., Yang, L., Yang, D.Q., & Sacher, E. (2022). Ag NP catalysis of Cu ions in the preparation of AgCu NPs and the mechanism of their enhanced antibacterial efficacy. *Colloids and Surfaces A: Physicochemical and Engineering Aspects*, 632: 127831. https://doi.org/10.1016/j.colsurfa.2021.127831